Geomagnetic anomaly associated with Fukushima earthquake on February 13th, 2021

Cipta Ramadhani[1*], *Bulkis* Kanata[1], *Abdullah* Zainuddin[1], *Rosmaliati*[1], and *Teti* Zubaidah[1]

[1]Dept Electrical Engineering, University of Mataram

Abstract. In this study, we performed research on electromagnetic anomalies related to earthquakes as early signs (precursors) that occurred in Fukushima, Japan on February 13th, 2021. The research focused on the utilization of geomagnetic field data which was derived from the Kakioka (KAK), Kanoya (KNY), and Memambetsu (MMB) observatories, particularly in the ultra-low frequency (ULF) to detect earthquake precursors. The method of electromagnetic data processing was conducted by applying a polarization ratio. In addition, we improved the methodology by splitting the ULF data (which ranged from 0.01-0.1 Hz) into 9 central frequencies and picking up the highest value from each central frequency to get the polarization ratio. The anomaly of magnetic polarization was identified 2-3 weeks before the mainshock in a narrowband frequency in the range of 0.04-0.05 Hz.

1 Introduction

Earthquakes are one of the deadliest natural disasters that occur suddenly and locally. Early signs (precursors) to detect the occurrence of an earthquake need to be conducted to reduce the hazard. Short-term earthquake forecasting gives promising results which have a time scale of about a week to a month before the event. Short-term earthquake forecasting can be potentially feasible by using geomagnetic disturbance observation instead of solely using seismometers. The weakness of using a seismometer is due to its limited sensitivity in detecting the generation of micro-fractures before an earthquake [1]. Therefore, research on electromagnetic anomalies related to earthquakes as precursors has attracted the attention of many researchers.

Geomagnetic emission in the range of ultra-low frequency provides a tremendous possibility for the detection of earthquake precursors since the emission of geomagnetic fields can propagate over the lithosphere layer of the earth with low attenuation. Thanks to the characteristic of a lithosphere layer that only damps high-frequency components instead of low-frequency components. Previous research has shown that disturbances in the geomagnetic field can be used to detect earthquakes, particularly in the ultra-low frequency (ULF) range [2]. The research began by Fraser-Smith et al [3], which reported the enhancement of geomagnetic noise at ULF 3 hours before the 1989 M7.1 Loa Prieta earthquake. Hayakawa et al [4] also reported that the anomalous variation in the vertical component of the geomagnetic field appeared 1 month before the 1995 Guam earthquake. Since then, geomagnetic earthquake forecasting studies have grown significantly.

Several studies have been conducted to monitor the activity of the earth's crust linked to electromagnetic anomalies within the limit of ULF (f<10 Hz) in terms of earthquake precursors. Previous studies have successfully shown that the ULF range within 0.01-0.1 Hz gave the best results for detecting electromagnetic anomalies in terms of earthquake precursors [5, 6, 7]. However, the ULF emission that can be assigned as electromagnetic anomalies has sometimes been problematic because not only is the intensity very weak (around 1nT) but it is usually difficult to understand as well due to the intense natural background of the geomagnetic field [8]. To distinguish between the emission and the background, polarization analysis has been applied to separate the vertical component of the geomagnetic field from the horizontal component [9, 10]. The Comparative Polarization signal for the H and Z components separates the ULF emission of solar wind, magnetosphere, ionosphere, or lithosphere and is derived from seismic origins [11].

The Geomagnetic Kp index is one of the most extensively used indices of geomagnetic activity. It has been used to monitor sub-auroral geomagnetic disturbance on a global scale which can indicate the occurrence of magnetic storms within the span of a day. For more than 70 years, the Kp index and derived products have shown their advantages, particularly for space weather research and service. The data set's integrity and future scientific and societal utilization are secured by a DOI [12] and the CC BY 4.0 license.

* Corresponding author: cipta.ramadhani@unram.ac.id

Table 1 The geographical positions of KNY, MMB, and KAK observatories

IAGA Code	Latitude	Longitude	Elevation(m)	Distance to EQ (km)
MMB	43.91 'N	144.19 'E	42	716
KAK	36.23 'N	140.18 'E	36	218
KNY	3.42 'N	130.88 'E	107	1217

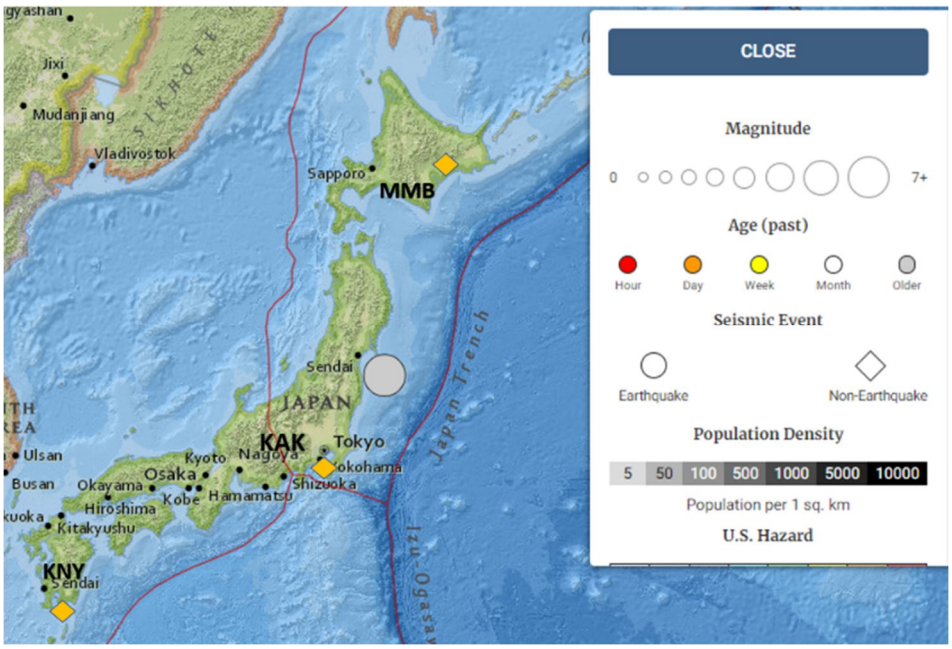

Fig. 1. The relative positions of KNY, MMB, and KAK observatories to the Earthquake (denoted by circles) that occurred on February 13th, 2021

In this paper, we tried to detect ULF geomagnetic precursors associated with the Fukushima earthquake on February 13th, 2021. The ULF data were derived from three different observatories from KAK, KNY, and MMB, which were closed from the earthquake event. The data from those observatories will be compared to each other to detect anomalies related to the earthquake precursor.

2 Methodology

2.1 Geomagnetic and Earthquake Data

The Fukushima earthquake with a magnitude of M7.1 occurred on Saturday, February 13th, 2021 at 14:07:49 (UTC) and has been reviewed by seismologists. The epicenter was located at 37.727°N, 141.775°E, at a depth of 44 km (27.3 miles). In the region near the east coast of Namie, Japan, 109 km (59 miles) ENE of Fukushima, Honshu, Japan.

The data was collected from three INTERMAGNET observatories in Japan, i.e. Kanoya (KNY), Memambetsu (MMB), and Kakioka (KAK). Table 1 shows the locations of the three observatories and their distances from the epicenter of the Fukushima earthquake, whereas Fig. 1 shows the epicenter and their locations of the Fukushima earthquake.

To reduce the influence of man-made noise, a shorter nigh local time of the geomagnetic data occurring between 00:00 to 00.03 PM (15:00 to 18:00 UTC) is used. For the analysis, a year's worth of statistical data is gathered, with seven months previous to and four months after the earthquake.

2.2 Frequency Range of ULF signal and Polarization Analysis.

2.2.1 Frequency Range of ULF Signal

In acquiring the frequency spectrum of the ULF signal, the Fast Fourier Transform (FFT) was applied with nine narrowband frequency ranges between 0.01 Hz and 0.10 Hz, which were Δf = 0.01 – 0.02, 0.02 – 0.03,..., 0.09 – 0.10 Hz [13]. The ULF signal in that narrowband frequency range is acquired by a bandpass filter. Furthermore, each selected range will be observed separately with polarization ratio analysis.

2.2.2 Polarization Analysis

The polarization ratio analysis approach is according to the observation of a daily precursor parameter called $P_{Z/H}$, which is the ratio of power spectral density (PSD) of the vertical component $S_Z(f)$ to PSD of the total horizontal

component $S_H(f)$. Both vertical and horizontal components were calculated using equation (1).

$$S_z(f) = \frac{|B_Z(f)|^2}{\Delta f}$$
$$S_H(f) = \frac{|B_H(f)|^2}{\Delta f} \quad (1)$$

where the highest value of ULF signals of $B_Z(f)$ and $B_Z(f)$ is selected in each narrow band. In addition, variable Δf is the difference between $f_{\text{up cut-off}}$ and $f_{\text{low cut-off}}$.

Furthermore, both vertical and horizontal components were normalized to certain ranges using equation (2). This equation was introduced by Yusuf, et al. [13] that successfully identified possible earthquake precursors in the equatorial and mid-latitudinal regions.

$$S_{X,norm} = \left(S_X - S_{X,max}\right)\left(\frac{M-m}{S_{X,max}-S_{X,min}}\right) + M \quad (2)$$

In the equation, X can be either Z (vertical) or H (horizontal) components, $S_{x,\ norm}$, and S_x are the normalized and authentic daily values of PSD of components X, respectively. $S_{X,\ max}$, and $S_{x,\ min}$ are the maximum and minimum PSD values of component X over the observation period. The terms M and m are upper and lower boundaries of the selected range, respectively; they are written as [m, M] for the rest of this paper. Based on the normalization process introduced by Yusuf et al. [13], the most effective way to detect precursor anomalies is to use [1,2] for S_H and [1,3] for S_Z as an upper and lower boundary respectively. The combination of the range values is useful because it not only prevents any daily value of S_H from being 0, thus avoiding an infinitely high $P_{Z/H}$, but also gives S_Z a higher proportion in determining the value of the corresponding $P_{Z/H}$ because Z is the most affected component due to crustal activities.

The next step is to calculate the ratio of $S_z(f)$ and $S_H(f)$ field components using equation (3).

$$P_{Z/H}(f) = \frac{S_z(f)}{S_H(f)} \quad (3)$$

Furthermore, to consider the increase of $P_{Z/H}$ anomalous in a given day in terms of statistics, its value must be greater than two standard deviations (σ) from the mean (μ) of the entire observation period:

$$P_{Z/H} > \mu + 2\sigma \quad (4)$$

2.3 The Kp Indices of Geomagnetic Activity.

To clearly explain the magnitude of geomagnetic activity in a single day, the Kp index provides information on the occurrence of magnetic storms within the period of each day. The Kp index is computed as a consequence of the impact of solar and other cosmic events. If the Kp index ≥ 5, the range value represented a geomagnetic storm; otherwise it is classified as calm. During a single day, the magnetic field recorded at the observatory can be interfered with by a high Kp index when a geomagnetic storm occurs.

3 Result and Discussion

In this section, we present the results of the polarization ratio analysis for the earthquake that occurred in Fukushima on February 13th, 2021. Fig. 2(a) represents the horizontal component ($S_H(f)$ of the Kakioka observatory. Meanwhile, Figs. 2(b) and 2(c) represent the vertical component ($S_z(f)$) and polarization ratio of $P_{Z/H}$, respectively. The Kp Index, which is used to determine the increase or decrease of the intensity of the magnetic field variations caused by solar activity or other phenomena, as shown in figure 2(d). The red shades denote disturbed periods where the Kp index surpassed the respective disturbed day thresholds (blue dashed lines in the figures). As previously stated, any anomalous $P_{Z/H}$ values during these periods were ignored. Furthermore, the content in figures 3 and 4 is identical to figure 2. However, they represent MMB and KNY observatories, respectively.

In all nine frequency ranges, the preliminary observation of normalized $P_{Z/H}$ was carried out. Nevertheless, they were not shown here. Instead, our focus was only on one frequency range that had an anomalous daily value and had the highest normalized value compared with the other frequency ranges.

By referring to figure 2, it was found that the range of 0.04-0.05 Hz had an apparent anomaly at the KAK observatory on 24 January 2021 (18 days before the Fukushima earthquake) with the intensity values as computed in Table 2. The normalized power spectral densities of $P_{Z/H}$ increased with a ratio of 2.3 (inside the red circle) and sigma Kp values of 10 (mean of Kp index=1.25), which means that there were no geomagnetic storms occurred throughout the anomalous period (no red shade denoted). It is acknowledged that there was an apparent second anomaly on January 11th, 2021 (31 days before the Fukushima earthquake). The normalized power spectral densities of $P_{Z/H}$ increased with a ratio of 2.16 (inside the red circle) and sigma Kp values of 18 (mean of Kp index=2.25). However, it was not considered as an earthquake precursor (it will be explained later). Both anomalous were seen higher than the respective disturbed day thresholds (blue dashed lines in the figures).

In the KNY observatory that appears in figure 3, it was anomaly signals with intensity values in the range of 0.04-0.05 Hz. Similar to the KAK observatory, it is acknowledged that there was an apparent anomaly on January 11th, 2021 with the intensity values as computed in Table 2. The normalized power spectral densities of $P_{Z/H}$ increased with a ratio of 2.39 (inside the red circle) and sigma Kp values of 18 (mean of Kp index=2.25). On the other hand, compared to the KAK observatory, it is acknowledged that there was a slight increment on January 24, 2021, that exceeded the respective thresholds (18 days before the Fukushima earthquake); nevertheless, but the excesses were minimal to meet the second criteria of being a precursor.

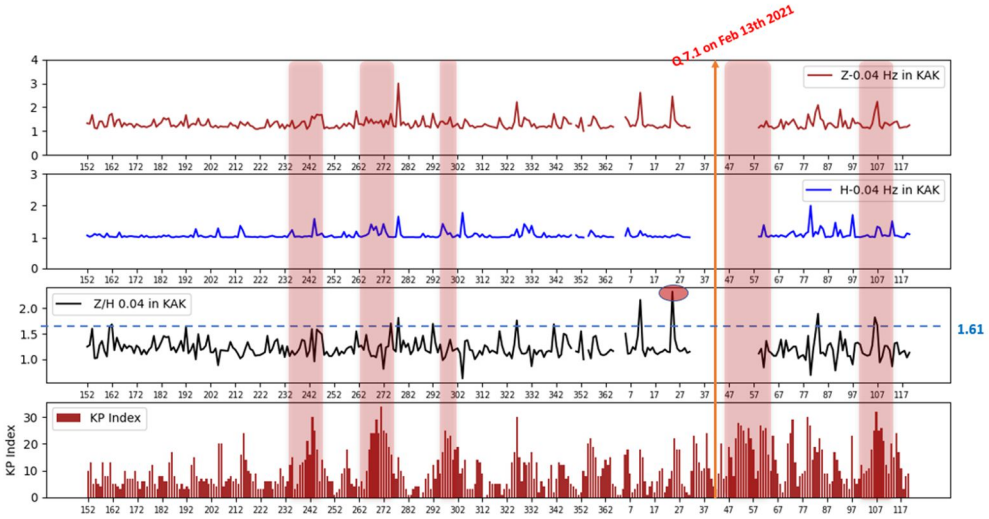

Fig. 2. Shows Power spectral densities of MMB observatory after normalization in the range of 0.04-0.05 Hz from June 1st, 2020 – May 30th, 2021, related to the M7.1 Fukushima earthquake on February 13th, 2021

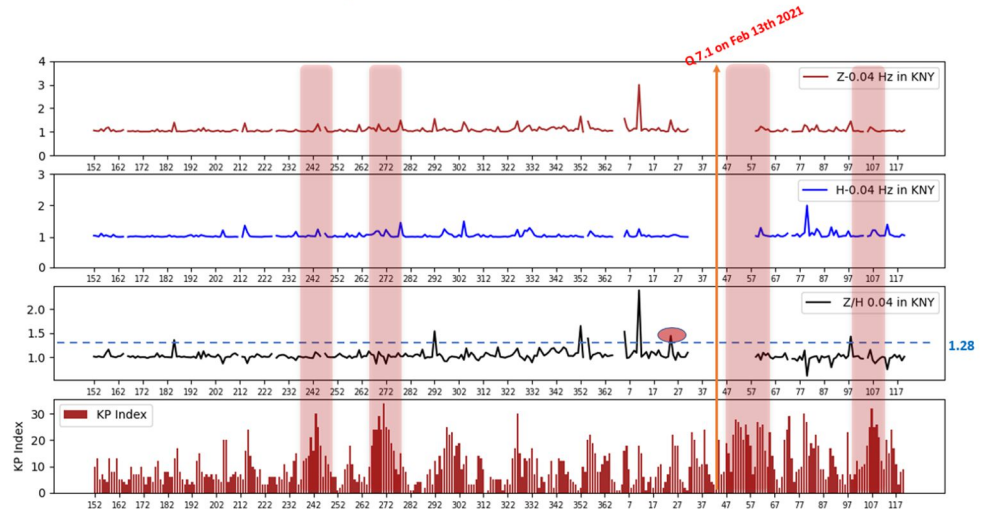

Fig. 3. Shows Power spectral densities of KNY observatory after normalization in the range of 0.04-0.05 Hz from June 1st, 2020 – May 30th, 2021, related to the M7.1 Fukushima earthquake on February 13th, 2021

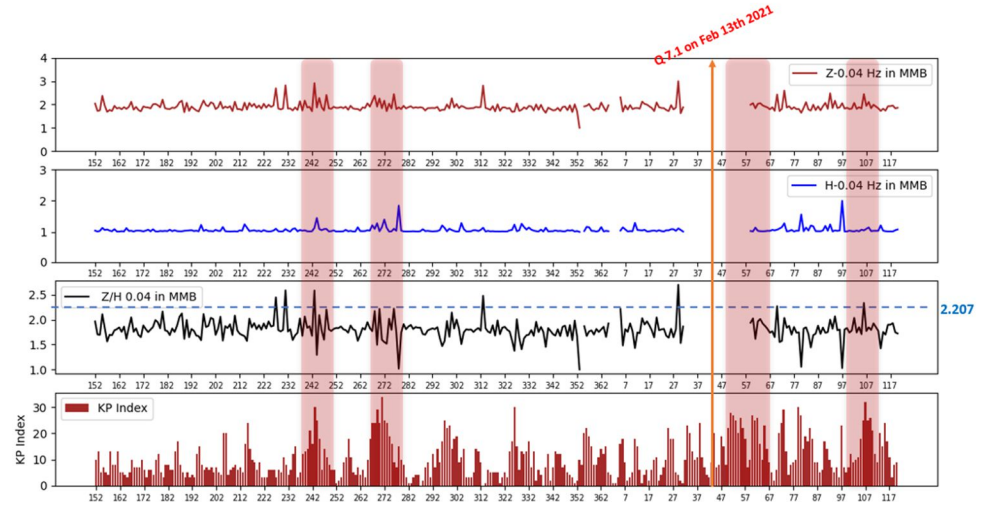

Fig. 4. Shows Power spectral densities of MMB observatory after normalization in the range of 0.04-0.05 Hz from June 1st, 2020 – May 30th, 2021, related to the M7.1 Fukushima earthquake on February 13th, 2021

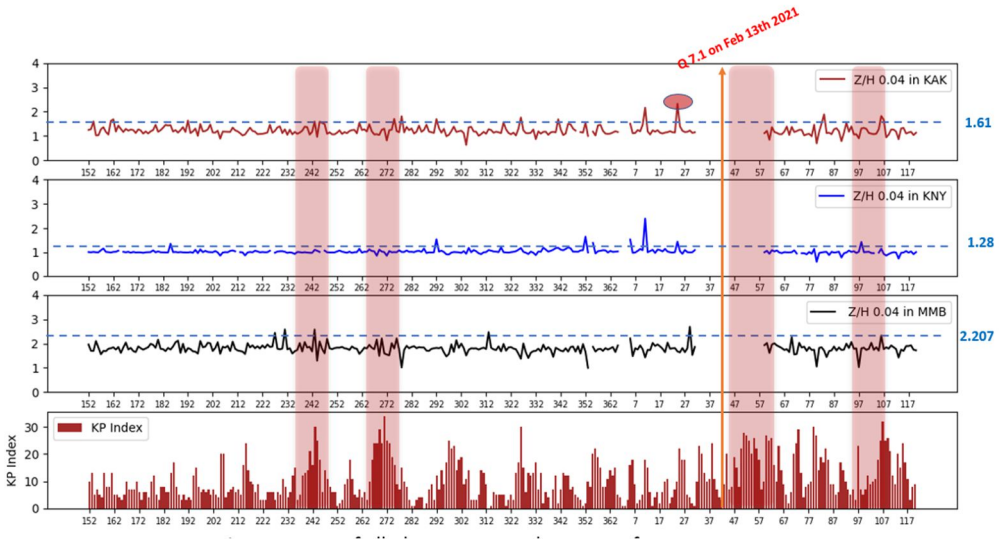

Fig. 5. Polarization ratio $P_{Z/H}$ of all observatories at the range of 0.04-0.05 Hz from June 1st, 2020 – May 30th, 2021, related to the M7.1 Fukushima earthquake on February 13th, 2021

Table 2 Characteristics of the identified anomalies preceding the main earthquakes obtained using normalized polarization ratio analysis at the range of 0.04-0.05 Hz

IAGA Code	Date of appearance	Lead time (days)	Normalized Value	Threshold	Sigma Kp
KAK	11/01/2021	31	2.162	1.61	18
	24/01/2021	18	2.322		10
KNY	11/01/2021	31	2.394	1.28	18
	24/01/2021	18	1.444		10
MMB	29/01/2021	13	2.695	2.207	22

Referring to figure 4, there were no anomalous signals at the MMB observatory on the same days that they appeared in KAK or KNY. However, it is acknowledged that there was a slight increment on January 29, 2021, with the intensity values as computed in Table 2. The normalized power spectral densities of $P_{Z/H}$ increased with a ratio of 2.6 and sigma Kp values 4 (mean of Kp index=0.2). Nevertheless, its value exceeded the respective thresholds (threshold =2.207), but the excesses were minimal to qualify as a precursor.

Figure 5 presented the results of all three observatories. Based on data, The KAK observatory provides the most visible indicators before the earthquake. This result implies that the closer an observatory is near the epicenter, the more anomalous data is recorded [14]. Based on these results, we suggest that the precursors can be noticed around three weeks (18 days) before an earthquake occurs. Based on the previous explanation, we refuse to admit the second anomaly from KAK and KNY observatories that appeared on January 11th, 2021 as an indicator before the Fukushima earthquake. Since The anomaly that appeared in both observatories did not appear in the MMB observatory. MMB observatory is closer than the KNY observatory. Therefore, if the anomaly appeared in the KNY observatory, it also appeared in the MMB observatory.

Despite the result, data for 27 days is not available from 1st February 2021 to 27th February 2021. Therefore, this research needs more evidence to make sure that the anomalies were relevant to being earthquake precursors.

4 Conclusion

This research discovered anomalous geomagnetic signals by using normalized polarization of Z/H in the narrowband frequency range of 0.04–0.05 Hz as a precursor to the Fukushima earthquake on February 13th, 2021. The anomalies are visible 2-3 weeks before the earthquake. In addition, the normalization process that was introduced by Yusof was enhanced in detecting ULF geomagnetic earthquake precursors by providing a significant proportion to the vertical component, since the vertical component is more affected by earthquake-related underground activities.

This research is funded by Universitas Mataram under Hibah Dana PNBP 2021 program entitled “Penerapan Metode Polarisasi Magnetik Untuk Analisis Prekursor Pada Kejadian Gempa Berskala Besar Di Fukushima Jepang”. The data that has been presented in this paper is collected from magnetic observatories. Our appreciation is presented to the national institutes and INTERMAGNET as their effort to promote high standards of magnetic observatory practice.

References

1. M. Hayakawa, *Earthquake prediction with electromagnetic phenomena*. AIP Conference Proceedings,**1709**, (2016)
2. F. Febriani, P. Han, C. Yoshino, K. Hattori, B. Nurdiyanto, N. Effendi, I. Maulana, Suhardjono, E. Gaffar, *Ultra-low frequency (ULF) electromagnetic anomalies associated with large earthquakes in Java Island, Indonesia by using wavelet transform and detrended fluctuation analysis*. Natural Hazards and Earth System Sciences, **14 (4)**, (2014)
3. A.C. Fraser-Smith, A. Bernardi, P.R. McGill, M.E. Ladd, R.A. Helliwell, O.G. Villard, *Low-frequency magnetic feld measurements near the epicenter of the Ms 7.1 Loma Prieta Earthquake*. GEOPHYSICAL RESEARCH LETTERS, **17 (9)**, 1465–1468, (1990)
4. M. Hayakawa, R. Kawate, O.A Molchanov, K. Yumoto, *Results of ultra-low-frequency magnetic feld measurements during the Guam earthquake of 8 August 1993*, Geophys Res Lett, **23**, 241–244 (1996)
5. C.H. Chen, C.H. Lin, C.H. Wang, J.Y. Liu, T.K. Yeh, H.Y. Yen, T.W. Lin, *Potential relationships between seismo-deformation and seismo-conductivity anomalies*. Journal of Asian Earth Sciences, **114**, 327–337 (2015)
6. G. Rawat, V. Chauhan, S. Dhamodharan, *Fractal dimension variability in ULF magnetic field with reference to local earthquakes at MPGO, Ghuttu*. Geomatics, Natural Hazards, and Risk, **7 (6)**, 1937–1947,(2016)
7. K.A. Yusof, M. Abdullah, N.S.A. Hamid, S. Ahadi, *On effective ULF frequency ranges for geomagnetic earthquake precursor*. Journal of Physics: Conference Series, **1152 (1)**, (2019)
8. N.R. Zalinskiy, N.G. Kleimenova, O.V Kozyreva, S.M. Agayan, S.R. Bogoutdinov, A.A. Soloviev, *Algorithm for recognizing Pc3 geomagnetic pulsations in 1-s data from INTERMAGNET equatorial observatories*. Izvestiya, Physics of the Solid Earth, **50 (2)**, 240–248 (2014)
9. J.L. Currie, C.L. Waters, *On the use of Geomagnetic indices and ULF waves for earthquake precursor signatures*, Journal of Geophysical Research A: Space Physics, **119 (2)**, 992–1003 (2014)
10. K.A. Yusof, N.S.A. Hamid, M. Abdullah, S. Ahadi, A. Yoshikawa, *Assessment of signal processing methods for the geomagnetic precursor of the 2012 M6.9 Visayas, Philippines earthquake*, Acta Geophysica, **67 (5)**, 1297–1306 (2019)
11. K. Yumoto and The MAGDAS Group, *MAGDAS Project and Its Application For Earthquake Prediction*, Proceedings of the International Workshop on Integration of Geophysical Parameter as a Set of Large Earthquake Precursors, Research and Development Center BMG, Jakarta (2006)
12. J. Matzka, O. Bronkalla, K. Tornow, K. Elger, C. Stolle, Geomagnetic Kp index, GFZ German Research Centre for Geosciences, 11 March, Potsdam, Germany,(2021)
13. K.A. Yusof, M. Abdullah, N. Shazan, A. Hamid, S. Ahadi, A. Yoshikawa, *Normalized Polarization Ratio Analysis for ULF Precursor Detection of the 2009 M7.6 Sumatra and 2015 M6.8 Honshu Earthquakes*, Jurnal Kejuruteraan, **3 (1),** 35-41 (2020)
14. B. Kanata, T. Zubaidah, C. Ramadhani, B. Irmawati, *Changes of the geomagnetic signals linked to Tohoku earthquake on March 11th, 2011*, International Journal of Technology, **5 (3)**, 251–258 (2014)